Eur. Phys. J. C (2016) 76:533
DOI 10.1140/epjc/s10052-016-4376-2

THE EUROPEAN PHYSICAL JOURNAL C



Regular Article - Theoretical Physics

# Measuring anomalous WW$\gamma$ and t$\bar{\text{t}}\gamma$ couplings using top+$\gamma$ production at the LHC

**Seyed Mohsen Etesami**[a], **Sara Khatibi, Mojtaba Mohammadi Najafabadi**

School of Particles and Accelerators, Institute for Research in Fundamental Sciences (IPM), P.O. Box 19395-5531, Tehran, Iran

Received: 11 June 2016 / Accepted: 15 September 2016 / Published online: 29 September 2016


**Abstract** We consider the electroweak production of a top quark in association with a photon at the LHC to probe the electroweak top quark couplings (t$\bar{\text{t}}\gamma$) as well as the triple gauge-boson couplings (WW$\gamma$). The study is based on the modifications of the t$\bar{\text{t}}\gamma$ and WW$\gamma$ interactions via heavy degrees of freedom in the form of dimension-six operators which we add to the standard model Lagrangian. A binned angular asymmetry in single top quark plus photon events and cross section ratio are proposed to probe the anomalous t$\bar{\text{t}}\gamma$ and WW$\gamma$ couplings. It is shown that the proposed angular asymmetry can distinguish anomalous t$\bar{\text{t}}\gamma$, WW$\gamma$ couplings from the standard model prediction and yield a great sensitivity.

## 1 Introduction

The standard model (SM) of particle physics has been found to be prosperous in explaining the strong and electroweak interactions. However, there are unanswered questions concerning possible SM extensions that incorporate new particles and new interactions. Studying top quark interactions and the electroweak gauge bosons self-interactions could provide applicable information in probing the extensions of the SM. As a result, precise measurements of the top quark interactions and the SM gauge-boson self-couplings are necessary since any deviation from the SM forms and values would be indicative of new physics beyond the SM. Anomalous triple gauge-boson couplings and the top quark interactions have been extensively studied in the literature; see for example [1–32] and the references therein.

A relevant approach in describing possible new physics effects is a model independent approach based on an effective field theory at low energy. In such an approach, all the heavy degrees of freedom are integrated out leading to obtain the effective interactions among the SM particles. This is justified due to the fact that the related observables have not shown any significant deviation from the SM predictions so far. These effective couplings are suppressed by the inverse powers of the new physics scale $\Lambda$. The effective Lagrangian is required to satisfy the SM local symmetry $SU(3)_C \times SU(2)_L \times U(1)_Y$. With the requirement of lepton and baryon number conservation, the Lagrangian takes the following form [33–35]:

$$\mathcal{L}_{eff} = \mathcal{L}_{SM} + \sum_i \frac{c_i O_i}{\Lambda^2} + h.c., \tag{1}$$

where $O_i$ are the gauge invariant operators of dimension-six and $c_i$ are the corresponding dimensionless coefficients. A list of dimension-six operators has been provided in [33–36]. Recently, discussions on the validity of the effective field theory extension of the SM with dimension-six operators and the fact that the validity range of the effective theory cannot be determined just based on the low energy information have been provided in [37].

The contributions from dimension-six operators including the SM coupling to the t$\bar{\text{t}}\gamma$ vertex is parameterized as follows [34]:

$$\mathcal{L}_{t\bar{t}\gamma} = -eQ_t\bar{t}\gamma^\mu t A_\mu - ie\bar{t}\frac{\sigma_{\mu\nu}q^\nu}{2m_t}\Big(\kappa + i\bar{\kappa}\gamma_5\Big)tA^\mu, \tag{2}$$

where the top quark charge and mass are denoted by $Q_t e$ and $m_t$, respectively. The CP even parameter $\kappa$ and CP odd parameter $\bar{\kappa}$ are related to the top quark anomalous magnetic ($a_t$) and electric ($d_t$) dipole moments via the following relations:

$$\kappa = Q_t a_t, \ \bar{\kappa} = \frac{2m_t}{e} d_t. \tag{3}$$

There two operators which contribute to the top quark anomalous magnetic and electric dipole moments [34]:

$$\mathcal{O}^{33}_{uB\phi} = \bar{q}_{L3}\sigma^{\mu\nu}t_R\tilde{\phi}B_{\mu\nu} + h.c. \quad \text{and}$$
$$\mathcal{O}^{33}_{uW} = \bar{q}_{L3}\sigma^{\mu\nu}\tau^a t_R\tilde{\phi}W^a_{\mu\nu} + h.c. \tag{4}$$

[a] e-mail: setesami@cern.ch

Based on the parameterization of Eq. 2 and using the operators introduced in Eq. 4, one finds

$$\kappa = \frac{2\sqrt{2}}{e}\frac{vm_t}{\Lambda^2}\mathrm{Re}\left[s_W C_{uW}^{33} + c_W C_{uB\phi}^{33}\right],$$
$$\tilde{\kappa} = \frac{2\sqrt{2}}{e}\frac{vm_t}{\Lambda^2}\mathrm{Im}\left[s_W C_{uW}^{33} + c_W C_{uB\phi}^{33}\right], \quad (5)$$

where $v = 246$ GeV and $s_W$ is the sine of the Weinberg angle. The prediction of the SM for the top quark anomalous magnetic dipole moment is $a_t = 0.02$, which corresponds to $\kappa = 0.013$ [38]. The CP violating electric dipole moment $d_t$ appears at three-loop level and is arising from the complex elements of the CKM matrix. It is found to be at the order of $d_t < 10^{-30} e$ cm corresponding to $\tilde{\kappa} < 5.7 \times 10^{-14}$ [39,40]. There are indirect constraints on the top quark magnetic and electric dipole moments from the b-quark rare decays $b \to s\gamma$ and the semi-leptonic b-quark decays [41,42]. The electric dipole moment, $d_t$, can also be constrained using the upper limit on the neutron electric dipole moment which was found to be $d_t < 3 \times 10^{-15} e$ cm [43]. The electric and magnetic dipole moments have also been probed using the direct $pp \to t\bar{t}\gamma$ production at the Tevatron and LHC. The combination of a direct probe and the related b-quark decays leads to the limits $a_t \in [-3, 0.45]$ and $d_t \in [-0.29, 0.86] \times 10^{-16} e$ cm [42]. The indirect constraint on the top quark electric dipole moment coming from the ThO electric dipole moment measurement has been found to be $5 \times 10^{-20} e$ cm [29].

In [44], the sensitivity of the single top quark production in association with a photon to the anomalous electric and magnetic dipole moments of the top quark has been examined. An analysis on the several kinematic distributions of this process leads to the constraints $a_t \in [-0.38, 0.39]$ and $d_t \in [-0.15, 0.15] \times 10^{-16} e$ cm at the LHC using 300 fb$^{-1}$ of integrated luminosity.

The dimension-six gauge invariant operators also contribute to the WW$\gamma$ coupling. Under the assumption of charge conjugation and parity invariance, the most general effective Lagrangian has the following form [45,46]:

$$\mathcal{L}_{WW\gamma} = -ie\left(W_{\mu\nu}^{\dagger} W^{\mu} A^{\nu} - W_{\mu}^{\dagger} A_{\nu} W^{\mu\nu}\right) + i\kappa_{\gamma} W_{\mu}^{\dagger} W_{\nu} F^{\mu\nu} + \frac{i\lambda}{m_W^2} W_{\alpha\beta}^{\dagger} W_{\delta}^{\beta} F^{\delta\alpha}, \quad (6)$$

where $m_W$ is the $W$ boson mass, $W_{\mu\nu} = \partial_{\mu} W_{\nu} - \partial_{\nu} W_{\mu}$. In the SM, at tree level $\kappa_{\gamma} = 1$ and $\lambda = 0$. At low energies, models with new heavy particles can effectively generate non-zero values for the anomalous triple gauge-boson couplings $\Delta\kappa_{\gamma}, \lambda$. These anomalous couplings $\lambda$ and $\Delta\kappa_{\gamma}$ (defined as $\kappa_{\gamma} - 1$) have been probed indirectly using rare b-quark decay ($b \to s\gamma$) [15] and directly at colliders [2,4]. At the LHC, W$\gamma$ production has been used to probe the anomalous WW$\gamma$ couplings. The 95 % CL limits on the anomalous couplings have been found to be $\Delta\kappa_{\gamma} \in [-0.38, 0.29]$ and $\lambda \in [-0.050, 0.037]$ from the CMS collaboration using 5 fb$^{-1}$ of proton–proton collisions at the center-of-mass energy of 7 TeV [47]. The ATLAS collaboration limits at the 95 % CL have been found to be $\Delta\kappa_{\gamma} \in [-0.41, 0.46]$ and $\lambda \in [-0.065, 0.061]$ with 4.6 fb$^{-1}$ of 7 TeV data [48]. In addition to the above results from the CMS and ATLAS collaborations, the anomalous triple gauge-boson couplings WW$\gamma$ have been studied at LEP [49] and Tevatron [50]. The anomalous triple gauge-boson couplings have also been confined by combining LEP data and the Higgs signal-strength data measured at the LHC experiments [31,51].

The aim of this paper is to explore the possibility of constraining the top quark dipole moments as well as the anomalous triple gauge-boson couplings WW$\gamma$ at the LHC through photon radiation in single top events in t-channel mode. We concentrate on the leptonic decay mode with $l = e, \mu$ and construct an angular asymmetry in single top quark plus photon events to study the anomalous $t\bar{t}\gamma$ and WW$\gamma$ couplings. We also consider the normalized cross section $\sigma_{tj\gamma}/\sigma_{tj}$ as a function of the anomalous couplings to set limits on those parameters.

The paper is organized as follows. In Sect. 2, single top quark production in association with a photon is introduced. In Sect. 3 the normalized cross section $\sigma_{tj\gamma}/\sigma_{tj}$ is suggested and examined to explore the anomalous couplings $t\bar{t}\gamma$ and WW$\gamma$. In Sect. 4, a binned angular asymmetry which increase the sensitivity to possible new physics effects is proposed. Finally, in Sect. 5, the summary and conclusions are given.

## 2 Single top quark production in association with a photon

At the LHC within the SM framework, single top quarks in association with a photon can be produced through three separate channels. These channels can be categorized based on the way of involvement of the W boson in the process. These processes are called t-, s- and tW-channels. In the t-channel process, the top quark is produced via the exchange of a virtual and space-like W boson. The involved W boson in s-channel top+$\gamma$ production is virtual and time-like while in the tW-channel the involved W boson is a real W boson. The t-channel process has the largest production rate at the LHC.

We explore the potential of the LHC for probing the top quark electric and magnetic dipole moments as well as the triple gauge-boson coupling WW$\gamma$ through photon radiation in single top events in the t-channel mode. The calculations are carried out at tree level and the decays of the top quark and $W$ boson are treated in narrow-width approximation. The photon radiation can occur in both top quark production and

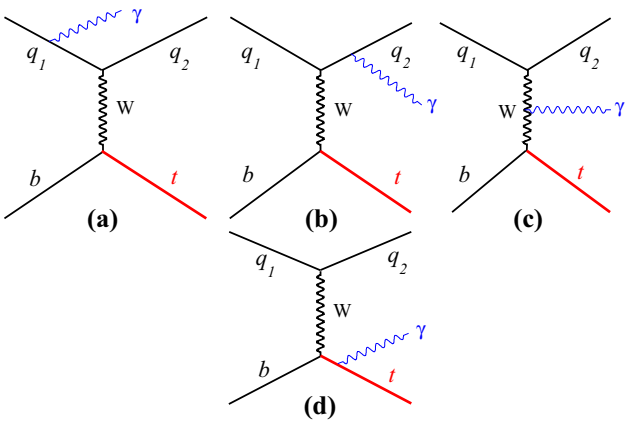


**Fig. 1** Representative leading-order Feynman diagrams for the process of $tj\gamma$ production

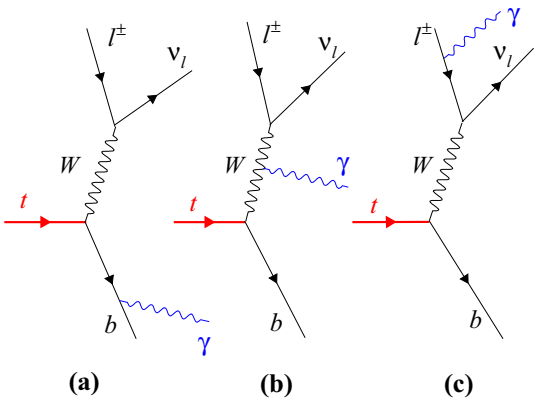


**Fig. 2** Additional Feynman diagrams contributing to $l\nu b\gamma$ production in proton–proton collisions at the LHC

top quark decay. As a result, the following processes have to be considered:

$$\begin{aligned} pp \to &\quad tj\gamma,\ t \to Wb \to l\nu b, \\ pp \to &\quad tj,\ t \to Wb\gamma \to l\nu b\gamma, \\ pp \to &\quad tj, t \to Wb,\ W \to l\nu\gamma. \end{aligned} \tag{7}$$

The Feynman diagrams contributing to the single top plus photon production are depicted in Fig. 1.

The additional Feynman diagrams corresponding to the cases that photon is emitted from the $W$ boson, b-quark and the charged lepton are presented in Fig. 2. In general, we cannot distinguish between the photon emission from top quark production and decay. As a result, the non-negligible interference effects between these two types need to be considered.

In order to perform numerical calculations and simulations we have chosen the SM input parameters to be: $m_t$ = 173.2 GeV, $m_W = 80.39$ GeV and $G_F = 1.16639 \times 10^{-5}$ GeV$^{-2}$. The event generation and cross section calculations are performed at leading order with MadGraph 5 [52,53] including the spin correlations for the subsequent decays of the top quark. We employ NNPDF3.0 [54] parton distribution functions and choose the value of the factorization and renormalization scales event-by-event to be $\mu_R = \mu_F = Q_0 = \sqrt{m_t^2 + \sum_i p_T^2(i)}$, where the sum is over the visible final state particles. All calculations are performed for proton–proton collisions at the center-of-mass energy of 13 TeV.

The cross section of process $pp \to t + j + \gamma$ becomes divergent when the emitted photon is collinear to the initial particle. In order to avoid such divergencies, we impose a minimum cut on the transverse momentum of the photon. To quantify the importance of contributions from the additional diagrams appearing in the top quark decays (Fig. 2), we compare the cross sections of $pp \to tj\gamma \times Br(t \to \mu\nu b)$ and $pp \to tj \to \mu\nu b\gamma$.

In Fig. 3, the cross sections of $pp \to tj\gamma \times Br(t \to \mu\nu b)$ and $pp \to tj \to \mu\nu b\gamma j$ are shown as a function of cut on the photon transverse momentum. The ratio $\sigma(\mu\nu b\gamma j)/\big(\sigma(tj\gamma) \times Br(t \to \mu\nu b)\big)$ is also calculated to show the importance of the new diagrams depicted in Fig. 2.

The cross sections and ratio are shown for two cases of angular separation between the photon and all other final state objects $\Delta R(X, \gamma) > 0.3$ and $\Delta R(X, \gamma) > 0.7$, where $\Delta R(X, \gamma) = \sqrt{(\eta_\gamma - \eta_X)^2 + (\phi_\gamma - \phi_X)^2}$. As can be seen, including the contributions where the photon is emitted from the decay products of the top quark leads to enhance the cross section by a factor of 1.5 when a minimum cut of 20 GeV is applied on the photon transverse momentum. The magnitudes of the cross sections and ratio decrease with increasing the minimum cut on the photon transverse momentum. The amplitudes of the Feynman diagrams presented in Fig. 2 are suppressed when we increase the cut on photon transverse momentum so that at a cut around 80 GeV, the cross sections are equal and the ratio tends to unity for $\Delta R(X, \gamma) > 0.3$. By comparing the left and right plots in Fig. 3 we observe that the cut at which the ratio is equal to one depends on $\Delta R(X, \gamma)$ cut and it decreases with increasing the cut on $\Delta R(X, \gamma)$. Applying a cut of 0.7 on the angular separation between photon and other final state particles $\Delta R(X, \gamma)$ leads to decrease the value of minimum $p_T$ cut at which the contribution of the additional Feynman diagrams, presented in Fig. 2, are quite suppressed.

## 3 Normalized cross section

The anomalous triple gauge-boson couplings WW$\gamma$ and the anomalous top quark dipole moments t$\bar{\text{t}}\gamma$ contribute to the single top quark production in association with a photon at the LHC. In particular, diagram (c) in Fig. 1 and diagram (b) in Fig. 2 are affected by the anomalous couplings WW$\gamma$. While the anomalous t$\bar{\text{t}}\gamma$ couplings only contribute to the single top plus photon production via diagram (d) in Fig. 1.

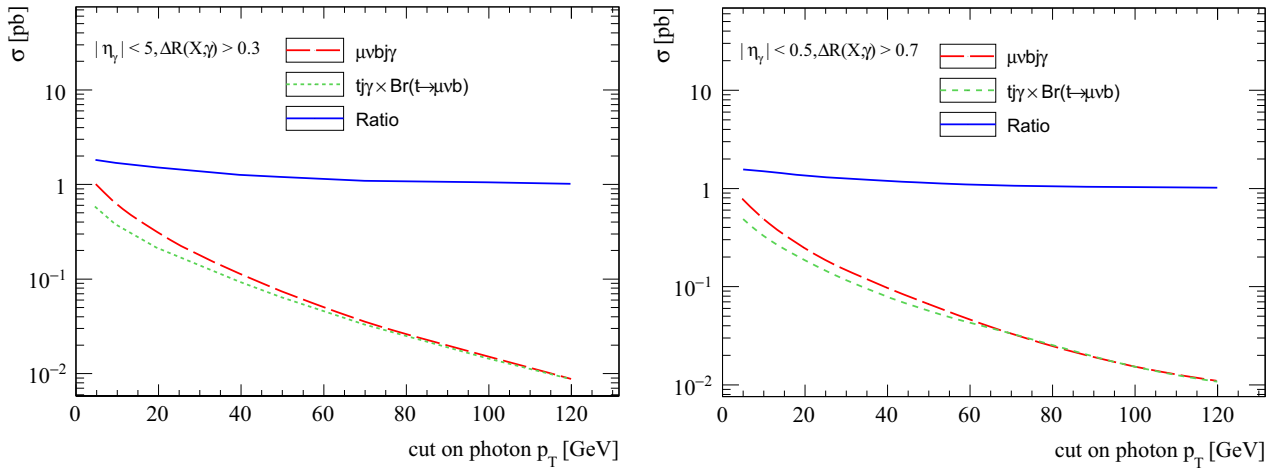


**Fig. 3** The cross section of $pp \to tj\gamma \times Br(t \to \mu\nu b)$ and $pp \to tj \to \mu\nu b\gamma$ as a function of cut on the photon transverse momentum and the ratio of the rates. The cross sections are presented with $\Delta R$ cuts of photon and other objects to be greater than 0.3 (*left*) and 0.7 (*right*)

In this section, we study the ratio between the production cross sections of $tj\gamma$ and $tj$, $R = \sigma_{tj\gamma}/\sigma_{tj}$, versus the anomalous couplings $\kappa$, $\tilde{\kappa}$, $\Delta\kappa_\gamma$, and $\lambda$ arising from the effective Lagrangians in Eqs. 2 and 6. The advantage of using the ratio $R$ is to relieve many experimental and theoretical sources of uncertainties with respect to the $tj\gamma$ production cross section. Experimental uncertainties such as jet energy scale, lepton identification, b-jet tagging, and luminosity are canceled out. While systematic uncertainties such as photon identification and acceptance uncertainties are not dropped out completely. The amount of theoretical uncertainty from the limited knowledge on parton distribution functions, variation of renormalization, and factorization scales are significantly reduced in the ratio with respect to the total production cross section. As a result, in [55,56], the CDF and CMS collaborations have measured the ratio between the top quark pair production in association with a photon and the top pair production rate. In [57], the authors have shown that the top quark Yukawa coupling can be measured with an uncertainty of 1 % using the measured ratio of $\sigma_{t\bar{t}H}/\sigma_{t\bar{t}Z}$ in proton–proton collisions at the future circular collider FCC-hh. This can be achieved due to the cancellation of several sources of the systematic uncertainties. Also, in [58] the authors make use of the ratio $\sigma_{tt\gamma}/\sigma_{t\bar{t}Z}$ to constrain the top quark electroweak dipole moments and show that there is a significant reduction of uncertainties in this ratio.

Now, we turn to study the effects of the anomalous couplings $\kappa$, $\tilde{\kappa}$, $\Delta\kappa_\gamma$, and $\lambda$ on the normalized cross section $R = \sigma_{tj\gamma}/\sigma_{tj}$. In order to perform the calculations and simulation, the effective Lagrangians, Eqs. 2 and 6, are implemented into the FeynRules [59] package and after that the model is exported to a Universal Feynrules Output (UFO) [60] module which is linked to MadGraph 5. Jets are reconstructed using the anti-k$_t$ [61] algorithm and b-tagging efficiency of 60 % is assumed for tagging the jets originating from the hadronization of b-quarks. We impose the following detector acceptance cuts on the transverse momentum, pseudorapidity, and angular separation:

$$\begin{aligned} p_{T,\gamma} &> 50\ \text{GeV},\ |\eta_\gamma| < 2.5\ ,\ E_{T,\text{miss}} > 20\ \text{GeV}, \\ p_{T,l} &> 20\ \text{GeV},\ |\eta_l| < 2.5, \\ p_{T,j,b} &> 20\ \text{GeV},\ \Delta R(m,n) > 0.4\ (m \neq n), \\ |\eta_b| &< 2.5,\ |\eta_j| < 5.0, \end{aligned} \tag{8}$$

where $m, n = \gamma, l, b, j$, $E_{T,\text{miss}}$ is the missing transverse energy and $\Delta R(m,n)$ is the separation between two particles $m$ and $n$ in the plane of pseudorapidity-azimuthal angle. In this study, no potential background processes are considered. The background processes to t-channel single top plus photon can be categorized into two classes: the irreducible and reducible background processes. The irreducible background process comes from the SM production of W$\gamma$+jets, which has a similar final state to the signal process. The reducible background processes originate from various SM processes that have different final state from the signal but show similar signature to single top quark in association with a photon because of misidentification of the final state objects. The main reducible background processes are W+jets and top pair events, with a jet misidentified as a photon. There are background processes with electrons from the decays of W and/or Z boson which are misidentified as photons in the detector. Z+jets process is an example of this type of backgrounds. Negligible background contributions can come from processes with di-lepton in the final state (such as Z($\to l^- l^+$)$\gamma$+jets) where one of the leptons is outside of detector coverage.

Since the SM prediction for the cross section of signal is small and there are many sources of background processes,

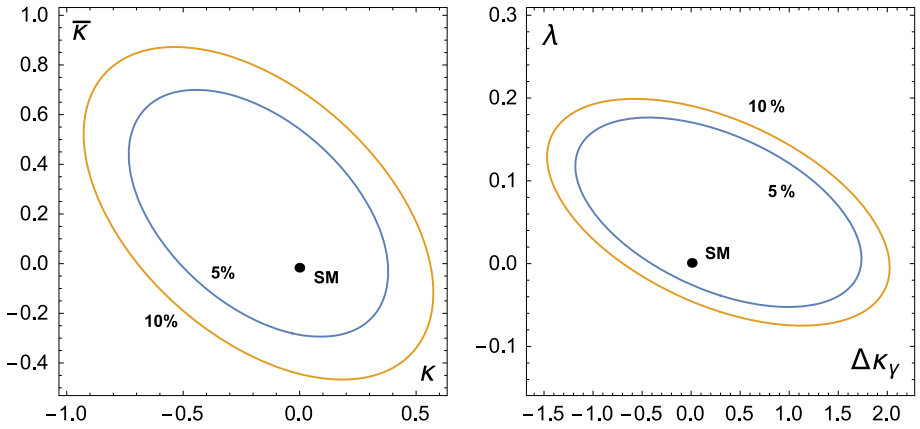


**Fig. 4** The 95 % CL contours in the plane of anomalous couplings $(\kappa, \bar{\kappa})$ (*left panel*) and $(\lambda, \Delta\kappa_\gamma)$ (*right panel*) corresponding to measurement of cross section ratio $R = \sigma_{tj+\gamma}/\sigma_{tj}$ are presented with assumed uncertainties of 5 and 10 %

it is necessary to increase as much as possible the separation between signal and background events. This would lead to the achievement of a good sensitivity to the anomalous couplings. In order to obtain the best discriminating power, a multivariate classification based on boosted decision trees (BDT) or neural network (NN) could be used [62]. Further improvement on this study would be to consider the detector effects as well as all background processes to have a more realistic estimate.

The leading-order SM prediction for the normalized cross section $R$ is found to be 0.27 %. We check the robustness of $R$ against variations of the renormalization and factorization scales and also the parton distribution functions. The ratio $R$ is calculated once with doubling and once with halving the scales, i.e. $\mu_R = \mu_F = Q_0/2$ and $\mu_R = \mu_F = 2 \times Q_0$. The changes on $R$ due to the variation of scales are found to be $+1.1$ and $-0.7$ %, corresponding to lowering and increasing the scales, respectively. To examine the stability of the ratio $R$ versus the variations of the parton distribution functions, three independent PDFs of NNPDF3.0 [54], CTEQ6L1 [63] and MRST [64] PDF sets are used to calculate the normalized cross section $R$. The change of the central value of $R$ due to using different PDFs is found to be less than 1 %, while the corresponding uncertainty on the total cross section of single top plus photon is around 3 %.

In order to obtain the sensitivity on the anomalous couplings using the normalized cross section $R$, we choose larger values than the uncertainties from the variation of renormalization and factorization scales and PDF. The results are presented with two assumed uncertainties of 5 and 10 % on measuring the normalized cross section $R$. Assuming such uncertainties are meaningful given that the LHC is going to deliver an anticipated integrated luminosity of around 300 $\text{fb}^{-1}$ in its Run 3 in which the statistical uncertainties in single top quark and single top quark plus photon processes are subdominant.

Figure 4 shows the 95 % CL contours for the anomalous top quark dipole couplings $\kappa$ and $\bar{\kappa}$ (left panel) and for the anomalous triple gauge couplings $\Delta\kappa_\gamma$ and $\lambda$ (right panel) with the assumed uncertainties of 5 and 10 % on $R$ measurement. With the uncertainty of 5, the 95 % CL bounds on the couplings are found to be $\kappa \in [-0.72, 0.38]$, $\bar{\kappa} \in [-0.27, 0.67]$, $\lambda \in [-0.05, 0.19]$, and $\Delta\kappa_\gamma \in [-1.1, 1.8]$. The limits on the anomalous dipole moments of the top quark $\kappa$ and $\bar{\kappa}$ are corresponding to the following limits on the electric and magnetic dipole moments of the top quark:

$$a_t \in [-1.08, 0.57] \text{ and } d_t \in [-1.54, 3.82] \times 10^{-17} e \text{ cm}. \tag{9}$$

For the electric and magnetic dipole moments, an improvement of around an order of magnitude is reachable in comparison with the constraints obtained from the combination of direct ($pp \to t\bar{t}\gamma$) and indirect ($b \to s\gamma$) searches mentioned previously. No considerable sensitivity is observed on the anomalous triple gauge-boson coupling $\Delta\kappa_\gamma$, while the lower bound on $\lambda$ is comparable with the one obtained from the W$\gamma$ process. In the next section, we suggest a particular angular asymmetry in single top quark production in association with a photon and examine its sensitivity to the anomalous couplings $\text{t}\bar{\text{t}}\gamma$ and WW$\gamma$.

## 4 Angular asymmetry

In this section, we construct an asymmetry from the kinematic observables of the final state particles of single top plus photon process to probe the anomalous $\text{t}\bar{\text{t}}\gamma$ and WW$\gamma$ couplings. The ability of this asymmetry to distinguish the contributions from the different Lorentz structures in the vertices of $\text{t}\bar{\text{t}}\gamma$ and WW$\gamma$ due to their particular characteristic momentum dependence is also investigated.

The presence of the anomalous $\text{t}\bar{\text{t}}\gamma$ is expected to affect the angular separation between the top quark and photon $\Delta R(t, \gamma)$ in single top quark production in association with a photon as well as other kinematic variables. It is also expected that the anomalous couplings WW$\gamma$ modify the angular distribution of the emitted photon as there are contributions

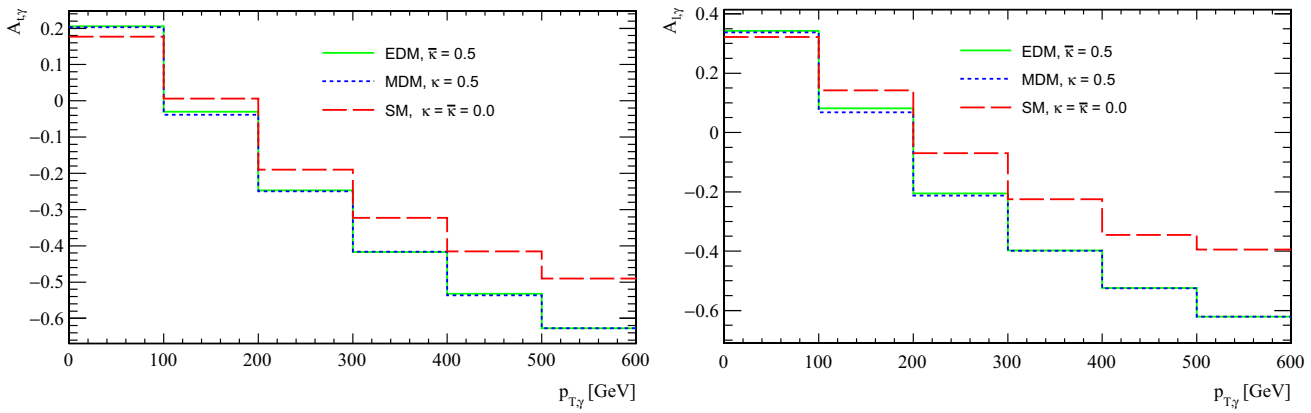


**Fig. 5** The dependence of the asymmetries on the photon $p_T$. The *left panel* shows the $A_{t,\gamma}(p_{T,\gamma})$ for the SM case and in the presence of *top* quark dipole moments while the $A_{l,\gamma}(p_{T,\gamma})$ is presented in the *right panel*. The *dashed red curve* depicts the SM case and the *solid green* and *dashed blue curves* show the asymmetries in the presence of $\kappa$ and $\tilde{\kappa}$

where the photon is radiated from the exchanged $W$ boson in both top quark production and decay. We consider the cosine of the angle between the top quark and photon, $\cos\left(\vec{p}_t, \vec{p}_\gamma\right)$, to construct the following asymmetry observable:

$$A_{t,\gamma} = \frac{N\big(\cos(\vec{p}_t, \vec{p}_\gamma) > 0\big) - N\big(\cos(\vec{p}_t, \vec{p}_\gamma) < 0\big)}{N\big(\cos(\vec{p}_t, \vec{p}_\gamma) > 0\big) + N\big(\cos(\vec{p}_t, \vec{p}_\gamma) < 0\big)}, \quad (10)$$

where $\vec{p}_t$ and $\vec{p}_\gamma$ are, respectively, the momentum vector of the top quark and photon in the lab frame. In this work, we look at this asymmetry with respect to the photon $p_T$ and calculate it in different bins of the photon transverse momentum. We choose the photon transverse momentum because from the experimental point of view it is a very clean object and easy to reconstruct. The distribution $A_{t,\gamma}(p_{T,\gamma})$ is shown in the left panel of Fig. 5. The dashed red curve shows the behavior of $A_{t,\gamma}(p_{T,\gamma})$ in the SM while the solid green and dashed blue curves show the asymmetries in the presence of electric and magnetic dipole moments, respectively.

The qualitative behavior of $A_{t,\gamma}(p_{T,\gamma})$ for the SM curve can be understood by looking at the distribution of $\cos\left(\vec{p}_t, \vec{p}_\gamma\right)$ in different bins of photon transverse momentum. Figure 6 shows the distributions of $\cos\left(\vec{p}_t, \vec{p}_\gamma\right)$ for the cases that $p_{T,\gamma} \in [50, 100]$, $[100, 200]$, $[200, 300]$, $[300, 400]$. As can be seen, photons with transverse momentum residing in the range of 50–100 GeV tend to be emitted mostly close to the top quark momentum direction. Going up to the higher momentum ranges leads to an increase of the probability for the photons to be radiated at large angles with respect to the top quark. This causes to have larger number of events with $\cos(\vec{p}_t, \vec{p}_\gamma) < 0$ as large photon $p_T$ is corresponding to emission with large angles with respect to the top quark. Higher photon transverse momentum is correlated with larger angles between the top and photon momenta. Therefore, the events with very high $p_T$ photon mostly tend

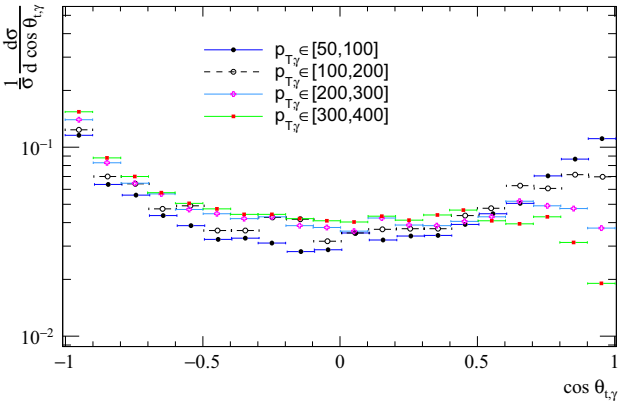


**Fig. 6** The normalized distribution of the cosine angle between the *top* quark and photon momenta in the lab frame in different bins of the photon transverse momentum predicted by the SM

to have $\cos(\vec{p}_t, \vec{p}_\gamma) < 0$. This causes $A_{t,\gamma}(p_{T,\gamma})$ to decrease with increasing photon transverse momentum.

There are reasons which motivate to use the cosine of the angle between the charged lepton and the photon $\cos(\vec{p}_l, \vec{p}_\gamma)$ instead of $\cos(\vec{p}_t, \vec{p}_\gamma)$ and consequently $A_{l,\gamma}$ as a reconstruction-independent asymmetry with the following definition instead of $A_{t,\gamma}$:

$$A_{l,\gamma} = \frac{N\big(\cos(\vec{p}_l, \vec{p}_\gamma) > 0\big) - N\big(\cos(\vec{p}_l, \vec{p}_\gamma) < 0\big)}{N\big(\cos(\vec{p}_l, \vec{p}_\gamma) > 0\big) + N\big(\cos(\vec{p}_l, \vec{p}_\gamma) < 0\big)}, \quad (11)$$

where $\vec{p}_l$ is the momentum vector of the charged lepton. The reasons that $A_{l,\gamma}$ is considered as an optimum observable with respect to $A_{t,\gamma}$ are as follows. First, $A_{l,\gamma}$ as a reconstruction-independent quantity has no combinatorial issues, therefore the sensitivity to the way of choosing the top decay products is significantly reduced. Second, $A_{l,\gamma}$ is less sensitive to modeling of the various distributions involved with respect to the $A_{t,\gamma}$ and consequently the related sys-

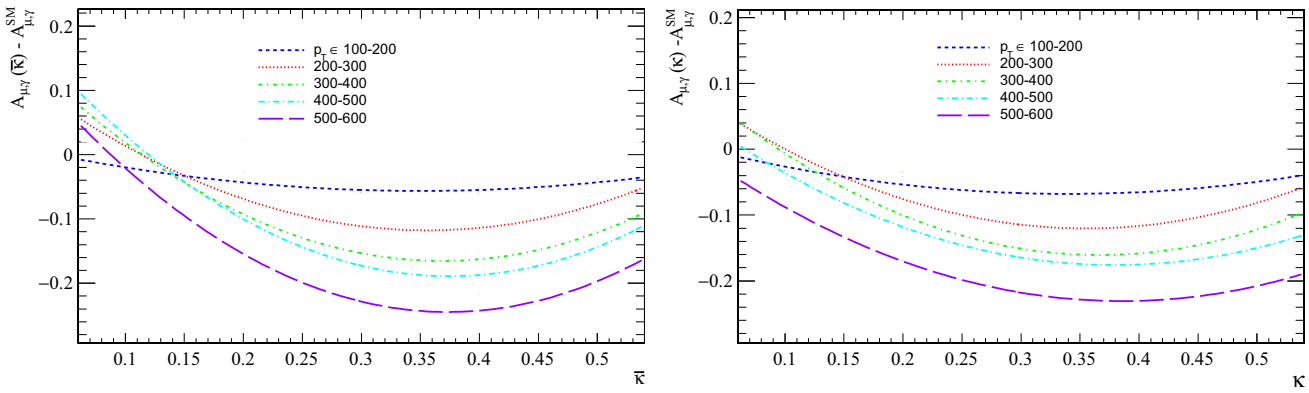


**Fig. 7** The dependence of difference of $A_{l,\gamma}(p_{T,\gamma})$ in the presence of the dipole moments from the SM value in various photon $p_T$ bins in terms of $\bar{\kappa}$ (*left panel*) and $\kappa$ (*right panel*) is shown

tematic uncertainties are under better control. The photon radiation coming from the top quark decay products changes the kinematics and smears the relation between $A_{t,\gamma}(p_{T,\gamma})$ and $A_{l,\gamma}(p_{T,\gamma})$. The behavior of $A_{l,\gamma}(p_{T,\gamma})$ is depicted in the right panel of Fig. 5.

As can be seen in Fig. 5, in the events with large photon $p_T$ the presence of electric and magnetic dipole moments for the top quark reduces the asymmetries from the SM predictions. This allows one to obtain the expected bounds on $\bar{\kappa}$ and $\kappa$. To this purpose, first we find the dependence of $A_{l,\gamma}(p_{T,\gamma})$ in the $p_T$ bins of photons. In Fig. 7, the dependence of the difference of $A_{l,\gamma}(p_{T,\gamma})$ in the presence of top quark dipole moments from the SM value is presented in various photon $p_T$ bins in terms of $\bar{\kappa}$ and $\kappa$. As expected, when we go to larger photon transverse momentum, larger deviations from the SM prediction are observed.

In order to obtain the sensitivity of the anomalous couplings a $\chi^2$ analysis is performed, where the sums of the variance of the asymmetry over all bins are computed. In the presence of new couplings, the $\chi^2$ is a function of the anomalous couplings $\kappa$ and $\bar{\kappa}$ and defined as

$$\chi^2(\kappa,\bar{\kappa}) = \sum_i^{n_{bin}} \left( \frac{A_{l,\gamma}(\kappa,\bar{\kappa})[i] - A^{\rm SM}_{l,\gamma}[i]}{\Delta A^{\rm SM}_{l,\gamma}[i]} \right)^2, \qquad (12)$$

where $A_{l,\gamma}(\kappa,\bar{\kappa})[i]$ and $A^{\rm SM}_{l,\gamma}[i]$ are the asymmetry predicted by the theory involving $\kappa$ and $\bar{\kappa}$ and the SM prediction for $i$th bin of photon transverse momentum. $\Delta A^{\rm SM}_{l,\gamma}[i]$ represents all sources of the uncertainties in $i$th bin of photon $p_T$. In this work, we only consider the statistical uncertainty which can be obtained using the following formula:

$$\Delta A^{\rm SM}_{l,\gamma} = \sqrt{\frac{1-(A^{\rm SM}_{l,\gamma})^2}{\sigma_{\rm SM}\times\mathcal{L}}}, \qquad (13)$$

where $\mathcal{L}$, $A_{\rm SM}$, and $\sigma_{\rm SM}$ are the integrated luminosity, the value of the asymmetry, and the cross section of the SM process, respectively. We perform the $\chi^2$ analysis on $A_{l,\gamma}(\kappa)$ and $A_{l,\gamma}(\bar{\kappa})$ distributions shown in the right panel of Fig. 5 to extract the upper limits separately on the anomalous couplings $\kappa$ and $\bar{\kappa}$ at 95 % CL. The results are shown in Table 1 for two different integrated luminosities 30 and 300 fb$^{-1}$.

**Table 1** The 95 % CL upper limits on the electric and magnetic dipole moments of the top quark obtained from single top+$\gamma$ channel at the LHC with the center-of-mass energy of 13 TeV and for integrated luminosities of 30 and 300 fb$^{-1}$

| Coupling | $\int \mathcal{L}dt = 30$ fb$^{-1}$ | $\int \mathcal{L}dt = 300$ fb$^{-1}$ |
|---|---|---|
| $d_t$ ($10^{-17}e$ cm) ($\bar{\kappa}$) | 1.2 (0.21) | 0.51 (0.09) |
| $a_t$ ($\kappa$) | 0.43 (0.29) | 0.16 (0.11) |

From Table 1, we see that with 30 fb$^{-1}$ the top quark electric and magnetic dipole moments could be probed down to the order of $10^{-17}e$ cm and 0.43, respectively. Using 300 fb$^{-1}$ integrated luminosity of data, the upper limit on the top quark magnetic dipole moment $a_t$ is found to be 0.16. This is still much larger than the SM prediction for $a_t$, which is 0.02.

Now, we turn to study the sensitivity of the proposed asymmetry $A_{l,\gamma}$ to the anomalous triple gauge-boson coupling WW$\gamma$ as introduced by the Lagrangian in Eq. 6. The distribution of $A_{l,\gamma}$ as a function of photon $p_T$ is shown in Fig. 8 for the SM, and for cases that anomalous WW$\gamma$ couplings are switched on. As expected the behavior of $A_{l,\gamma}(p_{T,\gamma})$ in the presence of $\kappa_\gamma$ is almost similar to the SM due to similarity in the couplings structure. However, the presence of anomalous coupling $\lambda$ distorts the shape of $A_{l,\gamma}(p_{T,\gamma})$ in particular at photon transverse momentum smaller than 200 GeV. As no significant deviation from the SM in the presence of $\Delta\kappa_\gamma$ is observed, very low sensitivity is expected to $\Delta\kappa_\gamma$. Following the same method as above leads to obtain upper limits on $\lambda$. The limits at 95 % CL on $\lambda$ are presented in Table 2. Comparing to the current limits from the CMS and ATLAS experiments, the limits are loose; however, this could

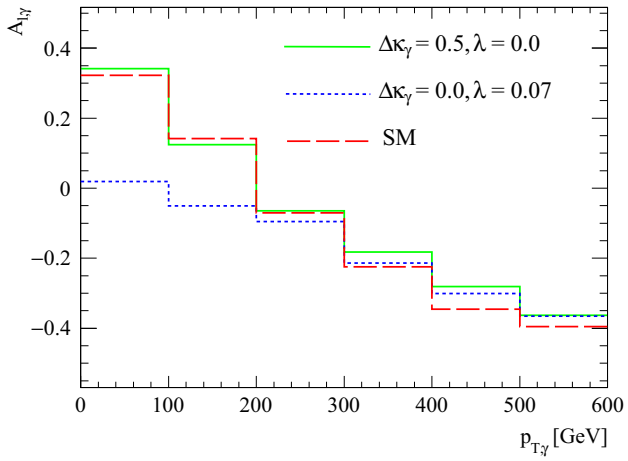


**Fig. 8** The dependence of the asymmetry $A_{l,\gamma}$ on the photon $p_T$. The plot shows $A_{l,\gamma}(p_{T,\gamma})$ for the SM case and in the presence of anomalous triple gauge-boson coupling WW$\gamma$. The *red dashed curve* depicts the SM case and the *solid green* and *dashed blue curves* show the asymmetries in the presence of $\Delta\kappa_\gamma$ and $\lambda$

**Table 2** The 95 % CL upper limits on the anomalous WW$\gamma$ couplings obtained from single top plus $\gamma$ channel at the LHC with the center-of-mass energy of 13 TeV and for integrated luminosities of 30 and 300 fb$^{-1}$

| Coupling | $\int \mathcal{L}dt = 30$ fb$^{-1}$ | $\int \mathcal{L}dt = 300$ fb$^{-1}$ |
|---|---|---|
| $\lambda$ | 0.22 | 0.065 |

be a complementary study to the W$\gamma$ channel for probing the anomalous triple gauge-boson couplings.

It is notable that in addition to t$\bar{\text{t}}\gamma$ and WW$\gamma$ anomalous couplings, single top plus photon production receives contributions from the anomalous Wtb vertex both in production and in decay. The most general effective Lagrangian describing the anomalous Wtb vertex has the following form [34]:

$$\mathcal{L}_{\text{Wtb}} = -\frac{g}{\sqrt{2}}\bar{b}\gamma^\mu(V_L P_L + V_R P_R)tW_\mu^- - \frac{g}{\sqrt{2}}\bar{b}\frac{i\sigma_{\mu\nu}q^\nu}{m_W}(g_L P_L + g_R P_R)tW_\mu^- + h.c. \quad (14)$$

where the coefficients $V_L$, $V_R$, $g_L$, and $g_R$ are dimensionless couplings. In the SM at tree level, $V_L = V_{tb}$ and other coefficients are equal to zero. The existing bounds on these anomalous couplings from the weak radiative B-meson decay are [65]: $-0.0007 < V_R < 0.0025$, $-0.0013 < g_L < 0.0004$, and $-0.15 < g_R < 0.57$. The constraints obtained at 95 % CL on the anomalous couplings from W boson helicities and t-channel cross section at the LHC are [66]: $-0.13 < V_R < 0.18$, $-0.09 < g_L < 0.06$, and $-0.15 < g_R < 0.01$. The normalized cross section $R = \sigma_{tj\gamma}/\sigma_{tj}$ introduced in Sect. 3 is found to be almost insensitive to the anomalous Wtb couplings as the dependency is canceled in the ratio. It is found that the variation of $g_{L,R}$ by an amount of 0.1 only leads to a change of around 0.1 % in $R$. The asymmetry observable $A_{l,\gamma}$ is found to also be insensitive to the anomalous Wtb couplings in both shape and magnitude. It has a similar behavior to the SM prediction in all bins of photon transverse momentum. As a result, $A_{l,\gamma}$ in single top production in association with a photon is an angular observable which can distinguish only between possible new physics originating from anomalous WW$\gamma$ interactions and top quark electric dipole moment.

## 5 Summary and conclusions

In this paper, we have investigated the possibility of measuring the non-standard couplings of t$\bar{\text{t}}\gamma$ and WW$\gamma$ through the process of single top quark production in association with a photon at the LHC. Our analysis is based on the effective Lagrangian approach in which the modifications of t$\bar{\text{t}}\gamma$ and WW$\gamma$ interactions are coming from the dimension-six operators. The analysis is carried out at leading order considering the processes in which the photon is either emitted in the production or from the top quark decay products.

We examined the sensitivity of the ratio between the production rates of $tj\gamma$ and $tj$ to the anomalous t$\bar{\text{t}}\gamma$ and WW$\gamma$. Many sources of the systematic uncertainties such as lepton and b-jet identification, jet energy scale, and luminosity uncertainties almost cancel in the ratio. Experimental uncertainties like photon identification and acceptance uncertainties are not canceled completely in the ratio. In particular, the leading-order calculations show that the systematic uncertainties originating from variations of scales and parton distribution functions on ratio $R$ is are the level of around 1 %. Based on assumed uncertainties of 5 and 10 % on measuring the normalized cross section $R$, constraints on the anomalous triple gauge-boson couplings WW$\gamma$ and t$\bar{\text{t}}\gamma$ are obtained. The bounds on the anomalous top quark dipole moments with an assumed conservative uncertainty of 5 % are found to be $a_t \in [-1.08, 0.57]$ and $d_t \in [-1.54, 3.82] \times 10^{-17} e$ cm. We find that the cross section ratio $R$ has a weak dependence on the anomalous coupling $\Delta\kappa_\gamma$ and therefore loose bounds are obtained. However, the strong lower bound $-0.05$ on another anomalous coupling $\lambda$ is reachable using the cross section ratio.

We also have defined a binned asymmetry observable using the distribution of the cosine angle between the charged lepton and photon as a tool to probe these new non-standard couplings. The asymmetry is calculated in the bins of the photon transverse momentum and has a descending behavior with increasing the photon transverse momentum. In our analysis, we have used a simple $\chi^2$ test in the absence of any systematic uncertainty to extract the sensitivity limits. Using the defined asymmetry, the sensitivity bounds on the anomalous electric and magnetic dipole moments can be sig-

nificantly strengthened. With 300 fb$^{-1}$ of data, the limits are found to be $|a_t| \leq 0.16$ and $|d_t| \leq 5.1 \times 10^{-18} e$ cm. The proposed asymmetry is found to be sensitive to only the anomalous gauge-boson coupling $\lambda$ and no significant sensitivity to $\Delta\kappa_\gamma$ is seen. An interesting observation is that the binned asymmetry has a discriminating capability between the SM and the anomalous couplings WW$\gamma$ and t$\bar{\text{t}}\gamma$ at the photon transverse momentum less than 200 GeV. Further improvements could be achieved including the higher-order corrections to the single top plus photon process in the presence of the anomalous couplings, considering the background processes and detector effects.

**Acknowledgments** Sara Khatibi is supported by Iranian National Science Foundation (INSF).



## References

1. T. Corbett, O.J.P. Éboli, J. Gonzalez-Fraile, M.C. Gonzalez-Garcia, Phys. Rev. Lett. **111**, 011801 (2013). doi:10.1103/PhysRevLett.111.011801. arXiv:1304.1151 [hep-ph]
2. D. Yang, Y. Mao, Q. Li, S. Liu, Z. Xu, K. Ye, JHEP **1304**, 108 (2013). doi:10.1007/JHEP04(2013)108. arXiv:1211.1641 [hep-ph]
3. J. Elias-Miró, C. Grojean, R.S. Gupta, D. Marzocca, JHEP **1405**, 019 (2014). doi:10.1007/JHEP05(2014)019. arXiv:1312.2928 [hep-ph]
4. L. Bian, J. Shu, Y. Zhang, JHEP **1509**, 206 (2015). doi:10.1007/JHEP09(2015)206. arXiv:1507.02238 [hep-ph]
5. S.D. Rindani, P. Sharma, A.W. Thomas, JHEP **1510**, 180 (2015). doi:10.1007/JHEP10(2015)180. arXiv:1507.08385 [hep-ph]
6. S.Y. Ayazi, H. Hesari, M.M. Najafabadi, Phys. Lett. B **727**, 199 (2013). doi:10.1016/j.physletb.2013.10.025. arXiv:1307.1846 [hep-ph]
7. S. Fayazbakhsh, S.T. Monfared, M.M. Najafabadi, Phys. Rev. D **92**(1), 014006 (2015). doi:10.1103/PhysRevD.92.014006. arXiv:1504.06695 [hep-ph]
8. S. Khatibi, M.M. Najafabadi, Phys. Rev. D **90**(7), 074014 (2014). arXiv:1409.6553 [hep-ph]
9. M.M. Najafabadi, J. Phys. G **34**, 39 (2007). arXiv:hep-ph/0601155
10. C. Englert, D. Goncalves, M. Spannowsky, Phys. Rev. D **89**(7), 074038 (2014). doi:10.1103/PhysRevD.89.074038. arXiv:1401.1502 [hep-ph]
11. W. Bernreuther, Z.G. Si, Phys. Lett. B **725**, 115 (2013). doi:10.1016/j.physletb.2013.06.051, 10.1016/j.physletb.2015.03.035. arXiv:1305.2066 [hep-ph] [erratum: Phys. Lett. B 744, 413 (2015)]
12. S.S. Biswal, S.D. Rindani, P. Sharma, Phys. Rev. D **88**, 074018 (2013). doi:10.1103/PhysRevD.88.074018. arXiv:1211.4075 [hep-ph]
13. C. Englert, A. Freitas, M. Spira, P.M. Zerwas, Phys. Lett. B **721**, 261 (2013). doi:10.1016/j.physletb.2013.03.017. arXiv:1210.2570 [hep-ph]
14. W. Bernreuther, D. Heisler, Z.G. Si, JHEP **1512**, 026 (2015). doi:10.1007/JHEP12(2015)026. arXiv:1508.05271 [hep-ph]
15. C. Bobeth, U. Haisch, JHEP **1509**, 018 (2015). doi:10.1007/JHEP09(2015)018. arXiv:1503.04829 [hep-ph]
16. K. Kolodziej, A. Slapik, Eur. Phys. J. C **75**(10), 475 (2015). doi:10.1140/epjc/s10052-015-3696-y. arXiv:1507.01572 [hep-ph]
17. Acta Phys, Polon. B **44**(8), 1775 (2013). doi:10.5506/APhysPolB.44.1775. arXiv:1212.6733 [hep-ph]
18. O.B. Bylund, F. Maltoni, I. Tsinikos, E. Vryonidou, C. Zhang, JHEP **1605**, 052 (2016). doi:10.1007/JHEP05(2016)052. arXiv:1601.08193 [hep-ph]
19. D. Atwood, S. Bar-Shalom, G. Eilam, A. Soni, Phys. Rept. **347**, 1 (2001). doi:10.1016/S0370-1573(00)00112-5. arXiv:hep-ph/0006032
20. G. Durieux, F. Maltoni, C. Zhang, Phys. Rev. D **91**(7), 074017 (2015). doi:10.1103/PhysRevD.91.074017. arXiv:1412.7166 [hep-ph]
21. J.A. Aguilar-Saavedra, B. Fuks, M.L. Mangano, Phys. Rev. D **91**, 094021 (2015). doi:10.1103/PhysRevD.91.094021. arXiv:1412.6654 [hep-ph]
22. J.A. Aguilar-Saavedra, N.F. Castro, A. Onofre, Phys. Rev. D **83**, 117301 (2011). doi:10.1103/PhysRevD.84.019901, 10.1103/PhysRevD.83.117301. arXiv:1105.0117 [hep-ph]
23. J.A. Aguilar-Saavedra, Nucl. Phys. B **804**, 160 (2008). doi:10.1016/j.nuclphysb.2008.06.013. arXiv:0803.3810 [hep-ph]
24. J.F. Kamenik, M. Papucci, A. Weiler, Phys. Rev. D **85**, 071501 (2012). doi:10.1103/PhysRevD.88.039903, 10.1103/PhysRevD.85.071501. arXiv:1107.3143 [hep-ph] [erratum: Phys. Rev. D 88(3), 039903 (2013)]
25. U. Baur, A. Juste, L.H. Orr, D. Rainwater, Phys. Rev. D **71**, 054013 (2005). doi:10.1103/PhysRevD.71.054013. arXiv:hep-ph/0412021
26. Z. Hioki, K. Ohkuma, Phys. Rev. D **88**, 017503 (2013). doi:10.1103/PhysRevD.88.017503. arXiv:1306.5387 [hep-ph]
27. A. Pomarol, F. Riva, JHEP **1401**, 151 (2014). doi:10.1007/JHEP01(2014)151. arXiv:1308.2803 [hep-ph]
28. T. Ibrahim, P. Nath, Phys. Rev. D **82**, 055001 (2010). doi:10.1103/PhysRevD.82.055001. arXiv:1007.0432 [hep-ph]
29. V. Cirigliano, W. Dekens, J. de Vries, E. Mereghetti, Phys. Rev. D **94**(1), 016002 (2016). doi:10.1103/PhysRevD.94.016002. arXiv:1603.03049 [hep-ph]
30. V. Cirigliano, W. Dekens, J. de Vries, E. Mereghetti, Phys. Rev. D **94**, 034031 (2016). doi:10.1103/PhysRevD.94.034031. arXiv:1605.04311 [hep-ph]
31. A. Butter, O.J.P. Éboli, J. Gonzalez-Fraile, M.C. Gonzalez-Garcia, T. Plehn, M. Rauch. arXiv:1604.03105 [hep-ph]
32. J.A. Aguilar-Saavedra, E. Álvarez, A. Juste, F. Rubbo, JHEP **1404**, 188 (2014). doi:10.1007/JHEP04(2014)188. arXiv:1402.3598 [hep-ph]
33. W. Buchmuller, D. Wyler, Nucl. Phys. B **268**, 621 (1986). doi:10.1016/0550-3213(86)90262-2
34. J.A. Aguilar-Saavedra, Nucl. Phys. B **812**, 181 (2009). arXiv:0811.3842 [hep-ph]
35. B. Grzadkowski, M. Iskrzynski, M. Misiak, J. Rosiek, JHEP **1010**, 085 (2010). doi:10.1007/JHEP10(2010)085. arXiv:1008.4884 [hep-ph]
36. C. Arzt, M.B. Einhorn, J. Wudka, Nucl. Phys. B **433**, 41 (1995). doi:10.1016/0550-3213(94)00336-D. arXiv:hep-ph/9405214
37. R. Contino, A. Falkowski, F. Goertz, C. Grojean, F. Riva. arXiv:1604.06444 [hep-ph]
38. W. Bernreuther, R. Bonciani, T. Gehrmann, R. Heinesch, T. Leineweber, P. Mastrolia, E. Remiddi, Phys. Rev. Lett. **95**, 261802 (2005). doi:10.1103/PhysRevLett.95.261802. arXiv:hep-ph/0509341
39. A. Soni, R.M. Xu, Phys. Rev. Lett. **69**, 33 (1992)
40. F. Hoogeveen, Nucl. Phys. B **341**, 322 (1990)

41. J.L. Hewett, T.G. Rizzo, Phys. Rev. D **49**, 319 (1994). doi:10.1103/PhysRevD.49.319. arXiv:hep-ph/9305223
42. A.O. Bouzas, F. Larios, Phys. Rev. D **87**(7), 074015 (2013). doi:10.1103/PhysRevD.87.074015. arXiv:1212.6575 [hep-ph]
43. A. Cordero-Cid, J.M. Hernandez, G. Tavares-Velasco, J.J. Toscano, J. Phys. G **35**, 025004 (2008). doi:10.1088/0954-3899/35/2/025004. arXiv:0712.0154 [hep-ph]
44. M. Fael, T. Gehrmann, Phys. Rev. D **88**, 033003 (2013). doi:10.1103/PhysRevD.88.033003. arXiv:1307.1349 [hep-ph]
45. K. Hagiwara, R.D. Peccei, D. Zeppenfeld, K. Hikasa, Nucl. Phys. B **282**, 253 (1987). doi:10.1016/0550-3213(87)90685-7
46. G. Gounaris et al. arXiv:hep-ph/9601233
47. S. Chatrchyan et al., CMS Collaboration, Phys. Rev. D **89**(9), 092005 (2014). doi:10.1103/PhysRevD.89.092005. arXiv:1308.6832 [hep-ex]
48. G. Aad et al., ATLAS Collaboration, Phys. Rev. D **87**(11), 112003 (2013). doi:10.1103/PhysRevD.87.112003, 10.1103/PhysRevD.91.119901. arXiv:1302.1283 [hep-ex] [erratum: Phys. Rev. D **91**(11), 119901 (2015)]
49. J. Alcaraz et al., ALEPH and DELPHI and L3 and OPAL and LEP Electroweak Working Group Collaborations. arXiv:hep-ex/0612034
50. V.M. Abazov et al., D0 Collaboration, Phys. Rev. D **71**, 091108 (2005). doi:10.1103/PhysRevD.71.091108. arXiv:hep-ex/0503048
51. A. Falkowski, M. Gonzalez-Alonso, A. Greljo, D. Marzocca, Phys. Rev. Lett. **116**(1), 011801 (2016). doi:10.1103/PhysRevLett.116.011801. arXiv:1508.00581 [hep-ph]
52. J. Alwall, M. Herquet, F. Maltoni, O. Mattelaer, T. Stelzer, JHEP **1106**, 128 (2011). doi:10.1007/JHEP06(2011)128. arXiv:1106.0522 [hep-ph]
53. J. Alwall et al., JHEP **1407**, 079 (2014). doi:10.1007/JHEP07(2014)079. arXiv:1405.0301 [hep-ph]
54. R.D. Ball et al., NNPDF Collaboration. JHEP **1504**, 040 (2015). doi:10.1007/JHEP04(2015)040. arXiv:1410.8849 [hep-ph]
55. T. Aaltonen et al., CDF Collaboration, Phys. Rev. D **84**, 031104 (2011). doi:10.1103/PhysRevD.84.031104. arXiv:1106.3970 [hep-ex]
56. CMS Collaboration [CMS Collaboration], CMS-PAS-TOP-13-011
57. M.L. Mangano, T. Plehn, P. Reimitz, T. Schell, H.S. Shao, J. Phys. G **43**(3), 035001 (2016). doi:10.1088/0954-3899/43/3/035001. arXiv:1507.08169 [hep-ph]
58. M. Schulze, Y. Soreq. arXiv:1603.08911 [hep-ph]
59. N.D. Christensen, C. Duhr, Comput. Phys. Commun. **180**, 1614 (2009). doi:10.1016/j.cpc.2009.02.018. arXiv:0806.4194 [hep-ph]
60. C. Degrande, C. Duhr, B. Fuks, D. Grellscheid, O. Mattelaer, T. Reiter, Comput. Phys. Commun. **183**, 1201 (2012). doi:10.1016/j.cpc.2012.01.022. arXiv:1108.2040 [hep-ph]
61. M. Cacciari, G.P. Salam, G. Soyez, JHEP **0804**, 063 (2008). doi:10.1088/1126-6708/2008/04/063. arXiv:0802.1189 [hep-ph]
62. B.P. Roe, H.J. Yang, J. Zhu, Y. Liu, I. Stancu, G. McGregor, Nucl. Instrum. Meth. A **543**(2–3), 577 (2005). doi:10.1016/j.nima.2004.12.018. arXiv:physics/0408124
63. J. Pumplin, D.R. Stump, J. Huston, H.L. Lai, P.M. Nadolsky, W.K. Tung, JHEP **0207**, 012 (2002). doi:10.1088/1126-6708/2002/07/012. arXiv:hep-ph/0201195
64. A.D. Martin, R.G. Roberts, W.J. Stirling, R.S. Thorne, Phys. Lett. B **531**, 216 (2002). doi:10.1016/S0370-2693(02)01483-1. arXiv:hep-ph/0201127
65. B. Grzadkowski, M. Misiak, Phys. Rev. D **78**(077501), 2008 (2011). doi:10.1103/PhysRevD.84.059903, 10.1103/PhysRevD.78.077501. arXiv:0802.1413 [hep-ph] [erratum: Phys. Rev. D **84**, 059903]
66. C. Bernardo, N.F. Castro, M.C.N. Fiolhais, H. Gonalves, A.G.C. Guerra, M. Oliveira, A. Onofre, Phys. Rev. D **90**(11), 113007 (2014). doi:10.1103/PhysRevD.90.113007. arXiv:1408.7063 [hep-ph]